Available online at www.sciencedirect.com
SCIENCE DIRECT®
Physics Letters B 547 (2002) 164–180
PHYSICS LETTERS B
www.elsevier.com/locate/npe

Inclusive jet cross sections in the Breit frame in neutral current deep inelastic scattering at HERA and determination of α_s

ZEUS Collaboration

S. Chekanov, D. Krakauer, S. Magill, B. Musgrave, J. Repond, R. Yoshida

Argonne National Laboratory, Argonne, IL 60439-4815, USA [1]

M.C.K. Mattingly

Andrews University, Berrien Springs, MI 49104-0380, USA

P. Antonioli, G. Bari, M. Basile, L. Bellagamba, D. Boscherini, A. Bruni, G. Bruni, G. Cara Romeo, L. Cifarelli, F. Cindolo, A. Contin, M. Corradi, S. De Pasquale, P. Giusti, G. Iacobucci, A. Margotti, R. Nania, F. Palmonari, A. Pesci, G. Sartorelli, A. Zichichi

University and INFN Bologna, Bologna, Italy [2]

G. Aghuzumtsyan, D. Bartsch, I. Brock, J. Crittenden [3], S. Goers, H. Hartmann, E. Hilger, P. Irrgang, H.-P. Jakob, A. Kappes, U.F. Katz [4], R. Kerger [5], O. Kind, E. Paul, J. Rautenberg [6], R. Renner, H. Schnurbusch, A. Stifutkin, J. Tandler, K.C. Voss, A. Weber

Physikalisches Institut der Universität Bonn, Bonn, Germany [7]

D.S. Bailey [8], N.H. Brook [8], J.E. Cole, B. Foster *, G.P. Heath, H.F. Heath, S. Robins, E. Rodrigues [9], J. Scott, R.J. Tapper, M. Wing

H.H. Wills Physics Laboratory, University of Bristol, Bristol, United Kingdom [10]

M. Capua, A. Mastroberardino, M. Schioppa, G. Susinno

Calabria University, Physics Department and INFN, Cosenza, Italy [2]

PII: S0370-2693(02)02763-6

J.Y. Kim, Y.K. Kim, J.H. Lee, I.T. Lim, M.Y. Pac [11]

Chonnam National University, Kwangju, South Korea [12]

A. Caldwell [13], M. Helbich, X. Liu, B. Mellado, Y. Ning, S. Paganis, Z. Ren, W.B. Schmidke, F. Sciulli

Nevis Laboratories, Columbia University, Irvington on Hudson, NY 10027, USA [43]

J. Chwastowski, A. Eskreys, J. Figiel, K. Olkiewicz, K. Piotrzkowski [15], M.B. Przybycień [16], P. Stopa, L. Zawiejski

Institute of Nuclear Physics, Cracow, Poland [17]

L. Adamczyk, T. Bołd, I. Grabowska-Bołd, D. Kisielewska, A.M. Kowal, M. Kowal, T. Kowalski, M. Przybycień, L. Suszycki, D. Szuba, J. Szuba [18]

Faculty of Physics and Nuclear Techniques, University of Mining and Metallurgy, Cracow, Poland [19]

A. Kotański [20], W. Słomiński [21]

Department of Physics, Jagellonian University, Cracow, Poland

L.A.T. Bauerdick [22], U. Behrens, K. Borras, V. Chiochia, D. Dannheim, M. Derrick [23], G. Drews, J. Fourletova, A. Fox-Murphy, U. Fricke, A. Geiser, F. Goebel [13], P. Göttlicher [24], O. Gutsche, T. Haas, W. Hain, G.F. Hartner, S. Hillert, U. Kötz, H. Kowalski [25], G. Kramberger, H. Labes, D. Lelas, B. Löhr, R. Mankel, M. Martínez [22], I.-A. Melzer-Pellmann, M. Moritz, D. Notz, M.C. Petrucci [26], A. Polini, A. Raval, U. Schneekloth, F. Selonke [27], B. Surrow [28], H. Wessoleck, R. Wichmann [29], G. Wolf, C. Youngman, W. Zeuner

Deutsches Elektronen-Synchrotron DESY, Hamburg, Germany

A. Lopez-Duran Viani [30], A. Meyer, S. Schlenstedt

DESY Zeuthen, Zeuthen, Germany

G. Barbagli, E. Gallo, C. Genta, P.G. Pelfer

University and INFN, Florence, Italy [2]

A. Bamberger, A. Benen, N. Coppola, H. Raach

Fakultät für Physik der Universität Freiburg i.Br., Freiburg i.Br., Germany [7]

M. Bell, P.J. Bussey, A.T. Doyle, C. Glasman, S. Hanlon, S.W. Lee, A. Lupi, G.J. McCance, D.H. Saxon, I.O. Skillicorn

Department of Physics and Astronomy, University of Glasgow, Glasgow, United Kingdom [10]

I. Gialas

Department of Engineering in Management and Finance, Univ. of Aegean, Greece

B. Bodmann, T. Carli, U. Holm, K. Klimek, N. Krumnack, E. Lohrmann, M. Milite, H. Salehi, S. Stonjek [31], K. Wick, A. Ziegler, Ar. Ziegler

Hamburg University, Institute of Exp. Physics, Hamburg, Germany [7]

C. Collins-Tooth, C. Foudas, R. Gonçalo [9], K.R. Long, F. Metlica, D.B. Miller, A.D. Tapper, R. Walker

Imperial College London, High Energy Nuclear Physics Group, London, United Kingdom [10]

P. Cloth, D. Filges

Forschungszentrum Jülich, Institut für Kernphysik, Jülich, Germany

M. Kuze, K. Nagano, K. Tokushuku [32], S. Yamada, Y. Yamazaki

Institute of Particle and Nuclear Studies, KEK, Tsukuba, Japan [33]

A.N. Barakbaev, E.G. Boos, N.S. Pokrovskiy, B.O. Zhautykov

Institute of Physics and Technology of Ministry of Education and Science of Kazakhstan, Almaty, Kazakhstan

H. Lim, D. Son

Kyungpook National University, Taegu, South Korea [12]

F. Barreiro, O. González, L. Labarga, J. del Peso, I. Redondo [34], J. Terrón, M. Vázquez

Departamento de Física Teórica, Universidad Autónoma de Madrid, Madrid, Spain [35]

M. Barbi, A. Bertolin, F. Corriveau, A. Ochs, S. Padhi, D.G. Stairs, M. St-Laurent

Department of Physics, McGill University, Montréal, PQ, Canada H3A 2T8 [36]

T. Tsurugai

Meiji Gakuin University, Faculty of General Education, Yokohama, Japan

A. Antonov, P. Danilov, B.A. Dolgoshein, D. Gladkov, V. Sosnovtsev, S. Suchkov

Moscow Engineering Physics Institute, Moscow, Russia [37]

R.K. Dementiev, P.F. Ermolov, Yu.A. Golubkov, I.I. Katkov, L.A. Khein, I.A. Korzhavina, V.A. Kuzmin, B.B. Levchenko, O.Yu. Lukina, A.S. Proskuryakov, L.M. Shcheglova, N.N. Vlasov, S.A. Zotkin

Moscow State University, Institute of Nuclear Physics, Moscow, Russia [38]

C. Bokel, J. Engelen, S. Grijpink, E. Koffeman, P. Kooijman, E. Maddox, A. Pellegrino, S. Schagen, E. Tassi, H. Tiecke, N. Tuning, J.J. Velthuis, L. Wiggers, E. de Wolf

NIKHEF and University of Amsterdam, Amsterdam, Netherlands [39]

N. Brümmer, B. Bylsma, L.S. Durkin, J. Gilmore, C.M. Ginsburg, C.L. Kim, T.Y. Ling

Physics Department, Ohio State University, Columbus, OH 43210, USA [1]

S. Boogert, A.M. Cooper-Sarkar, R.C.E. Devenish, J. Ferrando, G. Grzelak, T. Matsushita, M. Rigby, O. Ruske [40], M.R. Sutton, R. Walczak

Department of Physics, University of Oxford, Oxford, United Kingdom [10]

R. Brugnera, R. Carlin, F. Dal Corso, S. Dusini, A. Garfagnini, S. Limentani, A. Longhin, A. Parenti, M. Posocco, L. Stanco, M. Turcato

Dipartimento di Fisica dell' Università and INFN, Padova, Italy [2]

E.A. Heaphy, B.Y. Oh, P.R.B. Saull [41], J.J. Whitmore [42]

Department of Physics, Pennsylvania State University, University Park, PA 16802, USA [43]

Y. Iga

Polytechnic University, Sagamihara, Japan [33]

G. D'Agostini, G. Marini, A. Nigro

Dipartimento di Fisica, Università 'La Sapienza' and INFN, Rome, Italy

C. Cormack [44], J.C. Hart, N.A. McCubbin

Rutherford Appleton Laboratory, Chilton, Didcot, Oxon, United Kingdom [10]

C. Heusch

University of California, Santa Cruz, CA 95064, USA [1]

I.H. Park

Department of Physics, Ewha Womans University, Seoul, South Korea

N. Pavel

Fachbereich Physik der Universität-Gesamthochschule Siegen, Germany

H. Abramowicz, A. Gabareen, S. Kananov, A. Kreisel, A. Levy

Raymond and Beverly Sackler Faculty of Exact Sciences, School of Physics, Tel-Aviv University, Tel-Aviv, Israel [45]

T. Abe, T. Fusayasu, S. Kagawa, T. Kohno, T. Tawara, T. Yamashita

Department of Physics, University of Tokyo, Tokyo, Japan [33]

R. Hamatsu, T. Hirose [27], M. Inuzuka, S. Kitamura [46], K. Matsuzawa, T. Nishimura

Tokyo Metropolitan University, Deptartment of Physics, Tokyo, Japan [33]

M. Arneodo [47], N. Cartiglia, R. Cirio, M. Costa, M.I. Ferrero, S. Maselli, V. Monaco, C. Peroni, M. Ruspa, R. Sacchi, A. Solano, A. Staiano

Università di Torino, Dipartimento di Fisica Sperimentale and INFN, Torino, Italy [2]

R. Galea, T. Koop, G.M. Levman, J.F. Martin, A. Mirea, A. Sabetfakhri

Department of Physics, University of Toronto, Toronto, ON, Canada M5S 1A7 [36]

J.M. Butterworth, C. Gwenlan, R. Hall-Wilton, T.W. Jones, M.S. Lightwood, J.H. Loizides [48], B.J. West

Physics and Astronomy Department, University College London, London, United Kingdom [10]

J. Ciborowski [49], R. Ciesielski [50], R.J. Nowak, J.M. Pawlak, B. Smalska [51], J. Sztuk [52], T. Tymieniecka [53], A. Ukleja [53], J. Ukleja, A.F. Żarnecki

Warsaw University, Institute of Experimental Physics, Warsaw, Poland [54]

M. Adamus, P. Plucinski

Institute for Nuclear Studies, Warsaw, Poland [54]

Y. Eisenberg, L.K. Gladilin [55], D. Hochman, U. Karshon

Department of Particle Physics, Weizmann Institute, Rehovot, Israel [56]

D. Kçira, S. Lammers, L. Li, D.D. Reeder, A.A. Savin, W.H. Smith

Department of Physics, University of Wisconsin, Madison, WI 53706, USA [1]

A. Deshpande, S. Dhawan, V.W. Hughes, P.B. Straub

Department of Physics, Yale University, New Haven, CT 06520-8121, USA [1]

S. Bhadra, C.D. Catterall, S. Fourletov, S. Menary, M. Soares, J. Standage

Department of Physics, York University, ON, Canada M3J 1P3 [36]

Received 23 August 2002; accepted 29 September 2002

Editor: W.-D. Schlatter

Abstract

Inclusive jet differential cross sections have been measured in neutral current deep inelastic e^+p scattering for boson virtualities $Q^2 > 125$ GeV^2. The data were taken using the ZEUS detector at HERA and correspond to an integrated luminosity of 38.6 pb^{-1}. Jets were identified in the Breit frame using the longitudinally invariant k_T cluster algorithm. Measurements of differential inclusive jet cross sections are presented as functions of jet transverse energy ($E^B_{T,\mathrm{jet}}$), jet pseudorapidity and Q^2, for jets with $E^B_{T,\mathrm{jet}} > 8$ GeV. Next-to-leading-order QCD calculations agree well with the measurements both at high Q^2 and high $E^B_{T,\mathrm{jet}}$. The value of $\alpha_s(M_Z)$, determined from an analysis of $d\sigma/dQ^2$ for $Q^2 > 500$ GeV^2, is $\alpha_s(M_Z) = 0.1212 \pm 0.0017(\mathrm{stat.})^{+0.0023}_{-0.0031}(\mathrm{syst.})^{+0.0028}_{-0.0027}(\mathrm{th.})$.

* Corresponding author.
E-mail address: b.foster@bristol.ac.uk (B. Foster).

[1] Supported by the US Department of Energy.

[2] Supported by the Italian National Institute for Nuclear Physics (INFN).

[3] Now at Cornell University, Ithaca, NY, USA.

[4] On leave of absence at University of Erlangen-Nürnberg, Germany.

[5] Now at Ministère de la Culture, de L'Enseignement Supérieur et de la Recherche, Luxembourg.

[6] Supported by the GIF, contract I-523-13.7/97.

[7] Supported by the German Federal Ministry for Education and Research (BMBF), under contract numbers HZ1GUA 2, HZ1GUB 0, HZ1PDA 5, HZ1VFA 5.

[8] PPARC advanced fellow.

[9] Supported by the Portuguese Foundation for Science and Technology (FCT).

[10] Supported by the Particle Physics and Astronomy Research Council, UK.

[11] Now at Dongshin University, Naju, South Korea.

[12] Supported by the Korean Ministry of Education and Korea Science and Engineering Foundation.

[13] Now at Max-Planck-Institut für Physik, München, Germany.

[14] Supported by the US National Science Foundation.

[15] Now at Université Catholique de Louvain, Louvain-la-Neuve, Belgium.

[16] Now at Northwestern Univ., Evanston, IL, USA.

[17] Supported by the Polish State Committee for Scientific Research, grant No. 620/E-77/SPUB-M/DESY/P-03/DZ 247/2000-2002.

[18] Partly supported by the Israel Science Foundation and the Israel Ministry of Science.

[19] Supported by the Polish State Committee for Scientific Research, grant No. 112/E-356/SPUB-M/DESY/P-03/DZ 301/2000-2002, 2 P03B 13922.

[20] Supported by the Polish State Committee for Scientific Research, grant No. 2 P03B 09322.

[21] Member of Dept. of Computer Science.

[22] Now at Fermilab, Batavia, IL, USA.

[23] On leave from Argonne National Laboratory, USA.

[24] Now at DESY group FEB.

[25] On leave of absence at Columbia Univ., Nevis Labs., NY, USA.

[26] Now at INFN Perugia, Perugia, Italy.

[27] Retired.

[28] Now at Brookhaven National Lab., Upton, NY, USA.

[29] Now at Mobilcom AG, Rendsburg-Büdelsdorf, Germany.

[30] Now at Deutsche Börse Systems AG, Frankfurt/Main, Germany.

[31] Now at Univ. of Oxford, Oxford, UK.

[32] Also at University of Tokyo.

[33] Supported by the Japanese Ministry of Education, Science and Culture (the Monbusho) and its grants for Scientific Research.

1. Introduction

Jet production in neutral current deep inelastic e^+p scattering at high Q^2 (where Q^2 is the negative of the square of the virtuality of the exchanged boson) provides a testing ground for the theory of the strong interaction between quarks and gluons, namely, quantum chromodynamics (QCD). In deep inelastic scattering (DIS), the predictions of perturbative QCD (pQCD) have the form of a convolution of matrix elements with parton distribution functions (PDFs) of the target hadron. The matrix elements describe the short-distance structure of the interaction and are calculable in pQCD at each order, whilst the PDFs contain the description of the long-distance structure of the target hadron.

The evolution of the PDFs with the scale at which they are probed is predicted in pQCD to follow a set of renormalisation group equations (DGLAP equations [1]). However, an explicit determination of the PDFs requires experimental input. A wealth of data from fixed-target [2] and collider [3,4] experiments has allowed an accurate determination of the proton PDFs [5–10]. Good knowledge of PDFs makes measurements of jet production in DIS a sensitive test of the pQCD predictions of the short-distance structure of the partonic interactions.

The hadronic final state in neutral current DIS may consist of jets of high transverse energy produced in the short-distance process as well as the remnant (beam jet) of the incoming proton. A jet algorithm should distinguish as clearly as possible between the beam jet and the hard jets. Working in the Breit frame [11] is preferred, since it provides a maximal separation between the products of the beam fragmentation and the hard jets. In this frame, the exchanged virtual boson (V^*, with $V^* = \gamma, Z$) is purely spacelike, with 3-momentum $\boldsymbol{q} = (0, 0, -Q)$. In the Born process, the virtual boson is absorbed by the struck quark, which is back-scattered with zero transverse momentum with respect to the V^* direction, whereas the beam jet follows the direction of the initial struck quark. Thus, the contribution due to the current jet in events from the Born process is suppressed by requiring the production of jets with high transverse energy in this frame. Jet production in the Breit frame is, therefore, directly sensitive to hard QCD processes, thus allowing direct tests of the pQCD predictions. The use of the k_T cluster algorithm [12] to define jets in the Breit frame facilitates the separation of the beam fragmentation and the hard process in the calculations [13].

At leading order (LO) in the strong coupling constant, α_s, the boson–gluon-fusion (BGF, $V^*g \to q\bar{q}$) and QCD-Compton (QCDC, $V^*q \to qg$) processes give rise to two hard jets with opposite transverse momenta. The calculation of dijet cross sections in pQCD at fixed order in α_s is hampered by infrared-sensitive regions, so that additional jet-selection criteria must be applied to make reliable predictions [14]. This com-

[34] Now at LPNHE Ecole Polytechnique, Paris, France.
[35] Supported by the Spanish Ministry of Education and Science through funds provided by CICYT.
[36] Supported by the Natural Sciences and Engineering Research Council of Canada (NSERC).
[37] Partially supported by the German Federal Ministry for Education and Research (BMBF).
[38] Supported by the Fund for Fundamental Research of Russian Ministry for Science and Education and by the German Federal Ministry for Education and Research (BMBF).
[39] Supported by the Netherlands Foundation for Research on Matter (FOM).
[40] Now at IBM Global Services, Frankfurt/Main, Germany.
[41] Now at National Research Council, Ottawa, Canada.
[42] On leave of absence at The National Science Foundation, Arlington, VA, USA.
[43] Supported by the US National Science Foundation.
[44] Now at Univ. of London, Queen Mary College, London, UK.
[45] Supported by the German–Israeli Foundation, the Israel Science Foundation, and by the Israel Ministry of Science.
[46] Present address: Tokyo Metropolitan University of Health Sciences, Tokyo 116-8551, Japan.
[47] Also at Università del Piemonte Orientale, Novara, Italy.
[48] Supported by Argonne National Laboratory, USA.
[49] Also at Łódź University, Poland.
[50] Supported by the Polish State Committee for Scientific Research, grant No. 2 P03B 07222.
[51] Now at The Boston Consulting Group, Warsaw, Poland.
[52] Łódź University, Poland.
[53] Supported by German Federal Ministry for Education and Research (BMBF), POL 01/043.
[54] Supported by the Polish State Committee for Scientific Research, grant No. 115/E-343/SPUB-M/DESY/P-03/DZ 121/2001-2002, 2 P03B 07022.
[55] On leave from MSU, partly supported by University of Wisconsin via the US–Israel BSF.
[56] Supported by the MINERVA Gesellschaft für Forschung GmbH, the Israel Science Foundation, the US–Israel Binational Science Foundation, the Israel Ministry of Science and the Benozyio Center for High Energy Physics.

plication is absent in the case of cross-section calculations for inclusive jet production.

This Letter presents measurements of several differential cross sections for the inclusive production of jets with high transverse energy in the Breit frame. The analysis is restricted to large values of Q^2, $Q^2 > 125\ \mathrm{GeV}^2$, and the jets were selected according to their transverse energies and pseudorapidities in the Breit frame; in the definition of the cross sections, no cut was applied to the jets in the laboratory frame. The measurements are compared to next-to-leading-order (NLO) QCD calculations [15] using currently available parameterisations of the proton PDFs. The jet selection used allows a reduction in the theoretical uncertainty of the NLO QCD calculations with respect to those of dijet production [16,17]. A QCD analysis of the inclusive jet cross sections has been performed, which yields a more precise determination of α_s than was previously possible at HERA [17–21].

2. Experimental set-up

The data sample used in this analysis was collected with the ZEUS detector at HERA and corresponds to an integrated luminosity of $38.6 \pm 0.6\ \mathrm{pb}^{-1}$. During 1996–1997, HERA operated with protons of energy $E_p = 820$ GeV and positrons of energy $E_e = 27.5$ GeV. The ZEUS detector is described in detail elsewhere [22,23]. The main components used in the present analysis are the central tracking detector [24], positioned in a 1.43 T solenoidal magnetic field, and the uranium-scintillator sampling calorimeter (CAL) [25]. The tracking detector was used to establish an interaction vertex. The CAL covers 99.7% of the total solid angle. It is divided into three parts with a corresponding division in the polar angle,[57] θ, as viewed from the nominal interaction point: forward (FCAL, $2.6^\circ < \theta < 36.7^\circ$), barrel (BCAL, $36.7^\circ < \theta < 129.1^\circ$), and rear (RCAL, $129.1^\circ < \theta < 176.2^\circ$). The smallest subdivision of the CAL is called a cell. Under test-beam conditions, the CAL relative energy resolution is $18\%/\sqrt{E(\mathrm{GeV})}$ for electrons and $35\%/\sqrt{E(\mathrm{GeV})}$ for hadrons. Jet energies were corrected for the energy lost in inactive material, typically about 1 radiation length, in front of the CAL. The effects of uranium noise were minimised by discarding cells in the inner (electromagnetic) or outer (hadronic) sections if they had energy deposits of less than 60 or 110 MeV, respectively. A three-level trigger was used to select events online [23].

The luminosity was measured using the Bethe–Heitler reaction $e^+p \to e^+\gamma p$ [26]. The resulting small-angle energetic photons were measured by the luminosity monitor, a lead-scintillator calorimeter placed in the HERA tunnel at $Z = -107$ m.

3. Data selection and jet search

Neutral current DIS events were selected offline using criteria similar to those reported previously [27]. The main steps are briefly discussed below.

The scattered-positron candidate was identified from the pattern of energy deposits in the CAL [28]. The energy (E'_e) and polar angle (θ_e) of the positron candidate were determined from the CAL measurements. The Q^2 variable was reconstructed from the double angle method (Q^2_{DA}) [29], which uses θ_e and an angle γ that corresponds, in the quark–parton model, to the direction of the scattered quark. The angle γ was reconstructed from the CAL measurements of the hadronic final state [29]. The following requirements were imposed on the data sample:

- a positron candidate of energy $E'_e > 10$ GeV. This cut ensured a high and well understood positron-finding efficiency and suppressed background from photoproduction events, in which the scattered positron escapes down the rear beampipe;
- $y_e < 0.95$, where $y_e = 1 - E'_e(1 - \cos\theta_e)/(2E_e)$. This condition removed events in which fake positron candidates were found in the FCAL;
- the total energy not associated with the positron candidate within a cone of radius 0.7 units in the pseudorapidity-azimuth (η–ϕ) plane around the positron direction should be less than 10% of the positron energy. This condition removed

[57] The ZEUS coordinate system is a right-handed Cartesian system, with the Z axis pointing in the proton beam direction, referred to as the "forward direction", and the X axis pointing left towards the centre of HERA. The coordinate origin is at the nominal interaction point. The pseudorapidity is defined as $\eta = -\ln(\tan\theta/2)$.

photoproduction and DIS events in which part of a jet was falsely identified as the scattered positron;
- for $30^\circ < \theta_e < 140^\circ$, the fraction of the positron energy within a cone of radius 0.3 units in the η–ϕ plane around the positron direction should be larger than 0.9; for $\theta_e < 30^\circ$, the cut was raised to 0.98. This condition removed events in which a jet was falsely identified as the scattered positron;
- the vertex position along the beam axis should be in the range $-38 < Z < 32$ cm;
- $38 < (E - p_Z) < 65$ GeV, where E is the total energy as measured by the CAL, $E = \sum_i E_i$, and p_Z is the Z-component of the vector $\boldsymbol{p} = \sum_i E_i \boldsymbol{r_i}$; in both cases the sum runs over all CAL cells, E_i is the energy of the CAL cell i and $\boldsymbol{r_i}$ is a unit vector along the line joining the reconstructed vertex and the geometric centre of the cell i. This cut removed events with large initial-state radiation and further reduced the background from photoproduction;
- $\not{p}_T/\sqrt{E_T} < 2.5$ GeV$^{1/2}$, where $\not{p}_T$ is the missing transverse momentum as measured with the CAL ($\not{p}_T \equiv \sqrt{p_X^2 + p_Y^2}$) and E_T is the total transverse energy in the CAL. This cut removed cosmic rays and beam-related background;
- no second positron candidate with energy above 10 GeV and energy in the CAL, after subtracting that of the two positron candidates, below 4 GeV. This requirement removed elastic Compton scattering events ($ep \to e\gamma p$);
- $Q^2_{DA} > 125$ GeV^2;
- $-0.7 < \cos\gamma < 0.5$. The lower limit avoided a region with limited acceptance due to the requirement on the energy of the scattered positron, whilst the upper limit was chosen to ensure good reconstruction of the jets in the Breit frame.

The longitudinally invariant k_T cluster algorithm [12] was used in the inclusive mode [30] to reconstruct jets in the hadronic final state both in data and in Monte Carlo (MC) simulated events (see Section 4). In data, the algorithm was applied to the energy deposits measured in the CAL cells after excluding those associated with the scattered-positron candidate. The jet search was performed in the pseudorapidity (η^B)-azimuth (ϕ^B) plane of the Breit frame. In the following discussion, $E^B_{T,i}$ denotes the transverse energy, η^B_i the pseudorapidity and ϕ^B_i the azimuthal angle of object i in the Breit frame. For each pair of objects (where the initial objects are the energy deposits in the CAL cells), the quantity

$$d_{ij} = \left[\left(\eta^B_i - \eta^B_j\right)^2 + \left(\phi^B_i - \phi^B_j\right)^2\right] \times \min\left(E^B_{T,i}, E^B_{T,j}\right)^2 \quad (1)$$

was calculated. For each individual object, the quantity $d_i = (E^B_{T,i})^2$ was also calculated. If, of all the values $\{d_{ij}, d_i\}$, d_{kl} was the smallest, then objects k and l were combined into a single new object. If, however, d_k was the smallest, then object k was considered a jet and was removed from the sample. The procedure was repeated until all objects were assigned to jets. The jet variables were defined according to the Snowmass convention [31]:

$$E^B_{T,\text{jet}} = \sum_i E^B_{T,i}, \qquad \eta^B_{\text{jet}} = \frac{\sum_i E^B_{T,i}\eta^B_i}{E^B_{T,\text{jet}}},$$
$$\phi^B_{\text{jet}} = \frac{\sum_i E^B_{T,i}\phi^B_i}{E^B_{T,\text{jet}}}. \quad (2)$$

This prescription was also used to determine the variables of the intermediate objects.

After reconstructing the jet variables in the Breit frame, the massless four-momenta were boosted into the laboratory frame, where the transverse energy ($E^L_{T,\text{jet}}$), the pseudorapidity (η^L_{jet}) and the azimuthal angle (ϕ^L_{jet}) of each jet were calculated. Energy corrections were then applied to the jets in the laboratory frame and propagated into the jet transverse energies in the Breit frame. In addition, the jet variables in the laboratory frame were used to apply additional cuts on the selected sample:

- events were removed from the sample if the distance of any of the jets to the positron candidate in the η–ϕ plane of the laboratory frame,
$$d = \sqrt{\left(\eta^L_{\text{jet}} - \eta_e\right)^2 + \left(\phi^L_{\text{jet}} - \phi_e\right)^2}, \quad (3)$$
was smaller than 1 unit. This requirement removed some background from photoproduction and improved the purity of the sample;
- events were removed from the sample if any of the jets was in the backward region of the detector ($\eta^L_{\text{jet}} < -2$). This requirement removed events in

which a radiated photon from the positron was misidentified as a hadronic jet in the Breit frame;
- jets with low transverse energy in the laboratory frame ($E^L_{T,\mathrm{jet}} < 2.5$ GeV) were not included in the final sample; this cut removed a small number of jets for which the uncertainty on the energy correction was large.

It should be noted that these cuts were applied to improve the efficiency and purity of the sample of jets and were not used to define the phase-space region of the cross-section measurements. The simulated events were used to correct these effects on the cross sections. In particular, the effects of the last two cuts were estimated to be smaller than 3%. The final data sample contained 8523 events with at least one jet satisfying $E^B_{T,\mathrm{jet}} > 8$ GeV and $-2 < \eta^B_{\mathrm{jet}} < 1.8$. With the above criteria, 5073 one-jet, 3262 two-jet, 182 three-jet and 6 four-jet events were found. Since the net transverse momentum of the hadronic final state in the Breit frame is zero, an event with a single jet, according to a given selection criterion, must contain at least one other jet balancing its transverse momentum; however, this jet will not necessarily satisfy the jet-selection criteria.

4. Monte Carlo simulation

Samples of events were generated to determine the response of the detector to jets of hadrons and the correction factors necessary to obtain the hadron-level jet cross sections. The generated events were passed through the GEANT 3.13-based [32] ZEUS detector- and trigger-simulation programs [23]. They were reconstructed and analysed by the same program chain as the data.

Neutral current DIS events were generated using the LEPTO 6.5 program [33] interfaced to HERACLES 4.5.2 [34] via DJANGO 6.2.4 [35]. The HERACLES program includes photon and Z exchanges and first-order electroweak radiative corrections. The QCD cascade was modelled with the colour-dipole model [36] by using the ARIADNE 4.08 program [37] and including the BGF process. The colour-dipole model treats gluons emitted from quark–antiquark (diquark) pairs as radiation from a colour-dipole between two partons. This results in partons that are not ordered in their transverse momenta. The CTEQ4D [5] proton PDFs were used. As an alternative, samples of events were generated using the model of LEPTO based on first-order QCD matrix elements plus parton showers (MEPS). For the generation of the samples with MEPS, the option for soft-colour interactions was switched off [38]. In both cases, fragmentation into hadrons was performed using the LUND [39] string model as implemented in JETSET 7.4 [40].

The jet search was performed on the MC events using the energy measured in the CAL cells in the same way as for the data. Using the sample of events generated with either ARIADNE or LEPTO-MEPS and after applying the same offline selection as for the data, a good description of the measured distributions for the kinematic and jet variables was found. The same jet algorithm was also applied to the hadrons (partons) to obtain the predictions at the hadron (parton) level. The MC programs were used to correct the measured cross sections for QED radiative effects.

5. NLO QCD calculations

The measurements were compared with NLO QCD ($\mathcal{O}(\alpha_s^2)$) calculations obtained using the program DISENT [15]. The calculations were performed in the $\overline{\mathrm{MS}}$ renormalisation and factorisation schemes using a generalised version [15] of the subtraction method [41]. The number of flavours was set to five and the renormalisation (μ_R) and factorisation (μ_F) scales were chosen to be $\mu_R = E^B_{T,\mathrm{jet}}$ and $\mu_F = Q$, respectively. The strong coupling constant, α_s, was calculated at two loops with $\Lambda^{(5)}_{\overline{\mathrm{MS}}} = 220$ MeV, corresponding to $\alpha_s(M_Z) = 0.1175$. The calculations were performed using the MRST99 [8] parameterisations of the proton PDFs. The jet algorithm described in Section 3 was also applied to the partons in the events generated by DISENT in order to compute the jet cross-section predictions. The results obtained with DISENT were cross-checked by using the program DISASTER++ [42]. The differences were always within 2% and typically smaller than 1% [43].

Since the measurements refer to jets of hadrons, whereas the NLO QCD calculations refer to partons, the predictions were corrected to the hadron level

using the MC models. The multiplicative correction factor ($C_{\rm had}$) was defined as the ratio of the cross section for jets of hadrons over that for jets of partons, estimated by using the MC programs described in Section 4. In order to estimate the uncertainty in the simulation of the fragmentation process, events were also generated using the HERWIG 6.3 [44] program, where the hadronisation is simulated by using a cluster model [45]. The mean of the ratios obtained with ARIADNE, LEPTO-MEPS and HERWIG was taken as the value of $C_{\rm had}$, since the three predictions were in good agreement. The value of $C_{\rm had}$ differs from unity by less than 10%, except in the backward region of the Breit frame where it differs by 20%.

The NLO QCD predictions were also corrected for the Z-exchange contribution by using LEPTO. The multiplicative correction factor was defined as the ratio of the cross section for jets of partons obtained with both photon and Z exchange over that obtained with photon exchange only. The correction is negligible for $Q^2 < 2000$ GeV^2 but reaches 17% in the highest-Q^2 region.

Several sources of uncertainty in the theoretical predictions were considered:

- the uncertainty on the NLO QCD calculations due to terms beyond NLO, estimated by varying μ_R between $E^B_{T,\rm jet}/2$ and $2E^B_{T,\rm jet}$, was $\sim \pm 5\%$;
- the uncertainty on the NLO QCD calculations due to that on $\alpha_s(M_Z)$ was estimated by repeating the calculations using two additional sets of proton PDFs, MRST99$\uparrow\uparrow$ and MRST99$\downarrow\downarrow$ [8], determined assuming $\alpha_s(M_Z) = 0.1225$ and 0.1125, respectively. The difference between the calculations using these sets and MRST99 was scaled by a factor of 60% to reflect the current uncertainty on the world average of α_s [46]. The resulting uncertainty in the cross sections was $\sim \pm 5\%$;
- the variance of the hadronisation corrections as predicted by ARIADNE, LEPTO-MEPS and HERWIG was taken as the uncertainty in this correction, which was typically less than 1%;
- the uncertainty on the NLO QCD calculations due to the statistical and correlated systematic experimental uncertainties of each data set used in the determination of the proton PDFs was calculated, making use of the results of an analysis [10] that provided the covariance matrix of the fitted PDF parameters and the derivatives as a function of Bjorken x and Q^2. The resulting uncertainty in the cross sections was typically 3%, reaching 5% in the high-$E^B_{T,\rm jet}$ region. To estimate the uncertainties on the cross sections due to the theoretical uncertainties affecting the extraction of the proton PDFs, the calculation of all the differential cross sections was repeated using a number of different parameterisations obtained under different theoretical assumptions in the DGLAP fit [10]. This uncertainty in the cross sections was typically 3%.

The total theoretical uncertainty was obtained by adding in quadrature the individual uncertainties listed above.

6. Systematic uncertainties

The following sources of systematic uncertainty were considered for the measured jet cross sections [43,47]:

- the uncertainty in the absolute energy scale of the jets was estimated to be $\pm 1\%$ for $E^L_{T,\rm jet} > 10$ GeV [48] and $\pm 3\%$ for lower $E^L_{T,\rm jet}$ values. The resulting uncertainty was $\sim 5\%$;
- the uncertainty in the absolute energy scale of the positron candidate was estimated to be $\pm 1\%$ [4]. The resulting uncertainty was less than 1%;
- the differences in the results obtained by using either ARIADNE or LEPTO-MEPS to correct the data for detector and QED effects were taken to represent systematic uncertainties. The uncertainty was typically smaller than 3%;
- the analysis was repeated using an alternative technique [49] to select the scattered-positron candidate. The uncertainty was less than 2%;
- the $E^L_{T,\rm jet}$ cut was raised to 4 GeV. The uncertainty was smaller than 1%;
- the cut in $\eta^L_{\rm jet}$ used to suppress the contamination due to photons falsely identified as jets in the Breit frame was set to -3 and to -1.5. The uncertainty was typically $\sim 1\%$;
- the uncertainty in the cross sections due to that in the simulation of the trigger and in the cuts used to select the data was typically less than 3%.

In addition, there was an overall normalisation uncertainty of 1.6% from the luminosity determination, which was not considered in the cross-section calculation.

The systematic uncertainties not associated with the absolute energy scale of the jets were added in quadrature to the statistical uncertainties and are shown on the figures as error bars. The uncertainty due to the absolute energy scale of the jets is shown separately as a shaded band in each figure, due to the large bin-to-bin correlation.

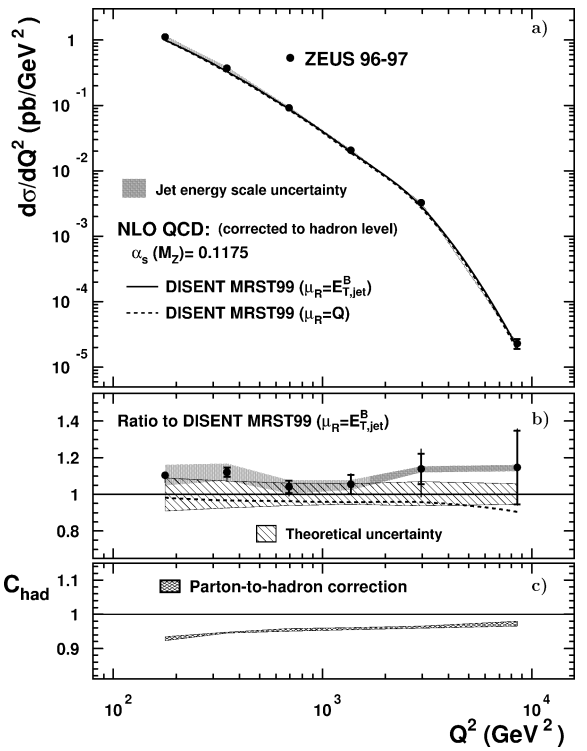

Fig. 1. (a) The differential cross-section $d\sigma/dQ^2$ for inclusive jet production with $E^B_{T,\mathrm{jet}} > 8$ GeV and $-2 < \eta^B_{\mathrm{jet}} < 1.8$ (filled dots). The inner error bars represent the statistical uncertainty. The outer error bars show the statistical and systematic uncertainties, not associated with the uncertainty in the absolute energy scale of the jets, added in quadrature. The shaded band displays the uncertainty due to the absolute energy scale of the jets. The NLO QCD calculations, corrected for hadronisation effects and using the MRST99 parameterisations of the proton PDFs, are shown for two choices of the renormalisation scale. (b) The ratio between the measured $d\sigma/dQ^2$ and the NLO QCD calculation; the hatched band displays the total theoretical uncertainty. The shaded band in (c) shows the magnitude and the uncertainty of the parton-to-hadron correction used to correct the NLO QCD predictions.

7. Inclusive jet differential cross sections

The differential inclusive jet cross sections were measured in the kinematic region $Q^2 > 125$ GeV^2 and $-0.7 < \cos\gamma < 0.5$. These cross sections include every jet of hadrons in the event with $E^B_{T,\mathrm{jet}} > 8$ GeV and $-2 < \eta^B_{\mathrm{jet}} < 1.8$ and were corrected for detector and QED radiative effects.

The measurements of the differential inclusive jet cross sections as functions of Q^2, $E^B_{T,\mathrm{jet}}$ and η^B_{jet} are presented in Figs. 1–3. The data points are plotted at the weighted mean in each bin of the corresponding variable as predicted by the NLO QCD calculation. The measured $d\sigma/dQ^2$ ($d\sigma/dE^B_{T,\mathrm{jet}}$) exhibits a steep fall-off over five (three) orders of magnitude in the Q^2 ($E^B_{T,\mathrm{jet}}$) range considered. In the low-Q^2 region ($125 < Q^2 < 250$ GeV^2), the selected data sample covers $3 \times 10^{-3} < x < 2 \times 10^{-2}$, whereas in the high-

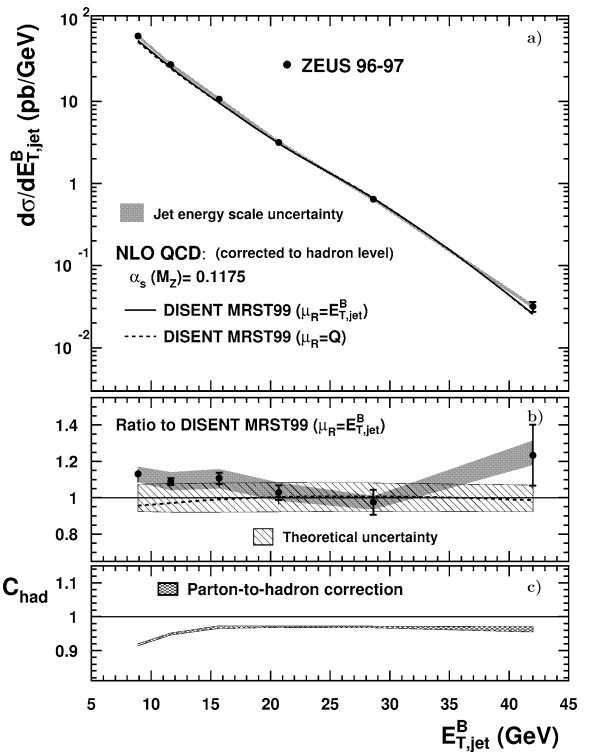

Fig. 2. (a) The differential cross-section $d\sigma/dE^B_{T,\mathrm{jet}}$ for inclusive jet production with $E^B_{T,\mathrm{jet}} > 8$ GeV and $-2 < \eta^B_{\mathrm{jet}} < 1.8$ (filled dots). Other details are as described in the caption to Fig. 1.

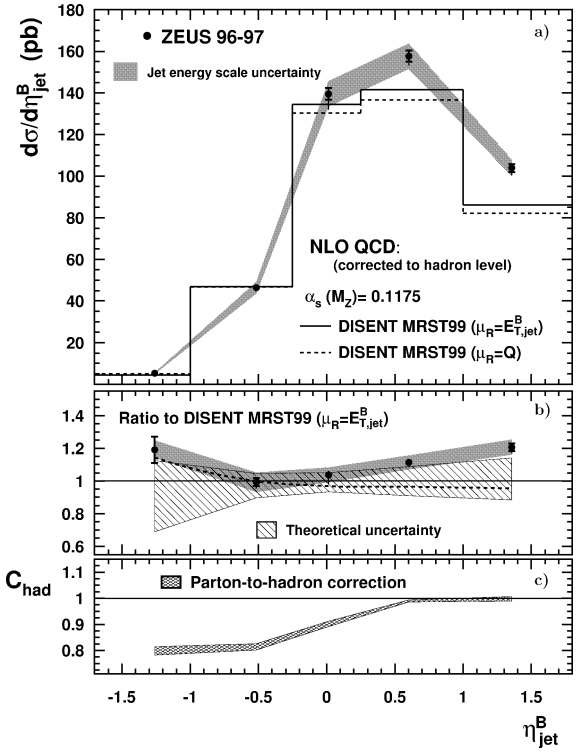

Fig. 3. (a) The differential cross-section $d\sigma/d\eta^B_{\rm jet}$ for inclusive jet production with $E^B_{T,\rm jet} > 8$ GeV and $-2 < \eta^B_{\rm jet} < 1.8$ (filled dots). Other details are as described in the caption to Fig. 1.

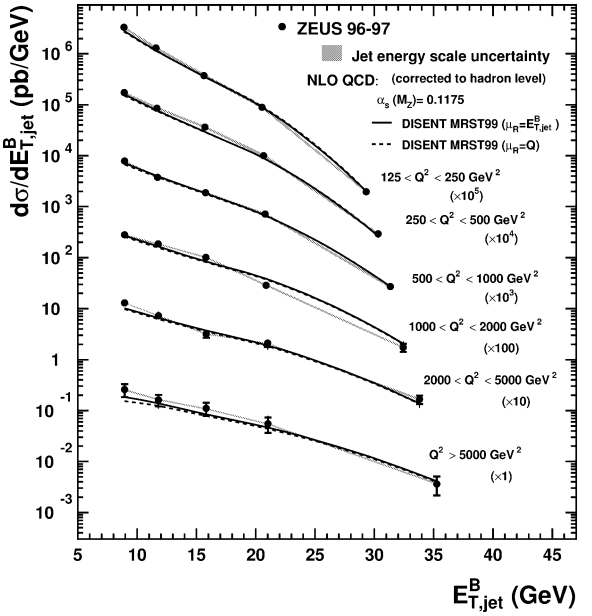

Fig. 4. The differential cross-section $d\sigma/dE^B_{T,\rm jet}$ for inclusive jet production with $E^B_{T,\rm jet} > 8$ GeV and $-2 < \eta^B_{\rm jet} < 1.8$ in different regions of Q^2 (filled dots). Each cross section has been multiplied by the scale factor indicated in brackets to aid visibility. Other details are as described in the caption to Fig. 1.

Q^2 region ($Q^2 > 5000\,\text{GeV}^2$), the range is $6\times10^{-2} < x < 0.25$.

The measurements of the differential cross-section $d\sigma/dE^B_{T,\rm jet}$ in different regions of Q^2 are presented in Fig. 4. The $E^B_{T,\rm jet}$ dependence of the cross section becomes less steep as Q^2 increases.

8. Comparison to NLO QCD calculations

The NLO QCD predictions, corrected as described in Section 5, are displayed and compared to the measurements in Figs. 1–4. It should be noted that the hadronisation correction, shown in Figs. 1(c), 2(c) and 3(c), was obtained with models (ARIADNE, LEPTO-MEPS and HERWIG) that implement higher-order contributions in an approximate way and, thus, their predictions do not constitute genuine fixed-order NLO QCD calculations. This procedure for applying hadronisation corrections to the NLO QCD calculations was verified by checking that the shapes of the calculated differential cross sections were well reproduced by the model predictions at the parton level.

The ratios of the measured differential cross sections over the NLO QCD calculations are shown in Figs. 1(b), 2(b), 3(b) and 5. The calculations reasonably reproduce the measured differential cross sections, although they tend to be below the data. The agreement observed at high Q^2 complements and extends an earlier comparison of the differential exclusive dijet cross sections at $Q^2 > 470$ GeV^2 [17]. For that measurement of the exclusive dijet cross sections, asymmetric cuts on the $E^B_{T,\rm jet}$ of the jets were applied [17] to avoid infrared-sensitive regions where NLO QCD programs are not reliable [14]. This difficulty is not present in the calculations of inclusive jet cross sections and, as a result, the theoretical uncertainties are smaller than in the dijet case. Thus, measurements of inclusive jet cross sections allow more precise tests of the pQCD predictions than dijet production.

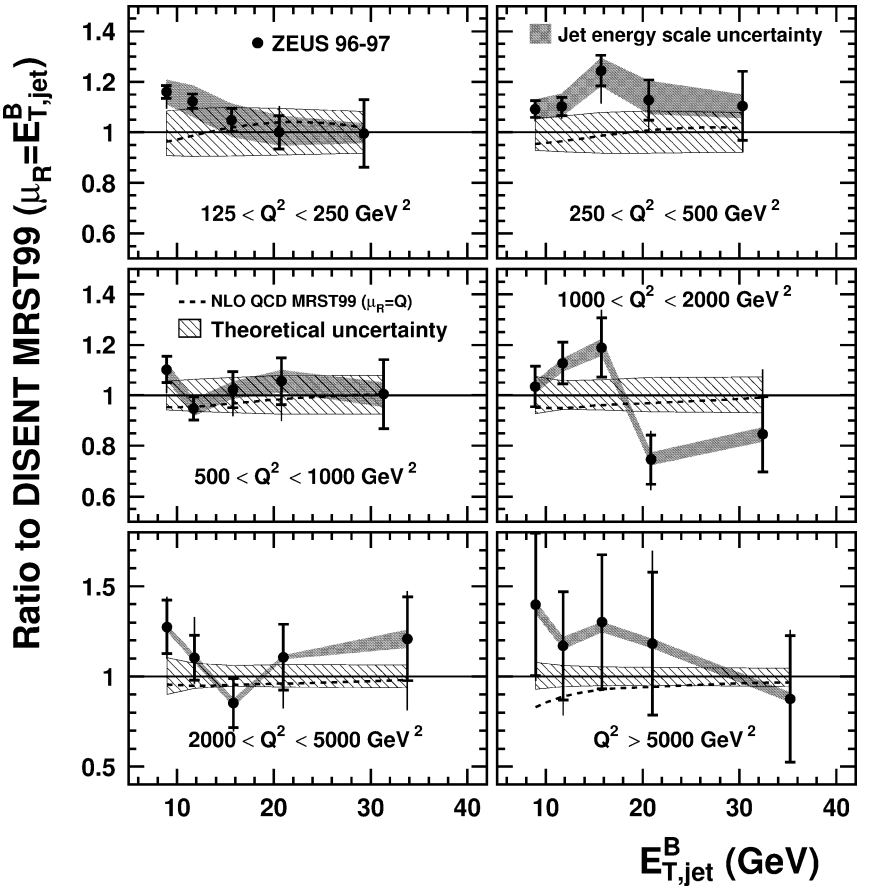

Fig. 5. Ratios between the differential cross-sections $d\sigma/dE^B_{T,\text{jet}}$ presented in Fig. 4 and NLO QCD calculations using the MRST99 parameterisations of the proton PDFs and $\mu_R = E^B_{T,\text{jet}}$ (filled dots). Other details are as described in the caption to Fig. 1.

At low Q^2 and low $E^B_{T,\text{jet}}$, the calculations fall below the data by ∼10%. The differences between the measurements and calculations are of the same size as the theoretical uncertainties. To study the scale dependence, NLO QCD calculations using $\mu_R = \mu_F = Q$, shown as the dashed line, are also compared to the data in Figs. 1–5; they provide a poorer description of the data than those using $\mu_R = E^B_{T,\text{jet}}$.

The overall description of the data by the NLO QCD calculations is sufficiently good to make a precise determination of α_s.

9. Measurement of α_s

The measured cross sections as a function of Q^2 and $E^B_{T,\text{jet}}$ were used to determine $\alpha_s(M_Z)$:

- NLO QCD calculations of $\frac{d\sigma}{dA}$ $(A = Q^2, E^B_{T,\text{jet}})$ were performed for the three MRST99 sets, central, $\alpha_s\uparrow\uparrow$ and $\alpha_s\downarrow\downarrow$. The value of $\alpha_s(M_Z)$ used in each partonic cross-section calculation was that associated with the corresponding set of PDFs;
- for each bin, i, in the variable A, the NLO QCD calculations, corrected for hadronisation effects, were used to parameterise the $\alpha_s(M_Z)$ dependence of $d\sigma/dA$ according to

$$\left[\frac{d\sigma}{dA}\big(\alpha_s(M_Z)\big)\right]_i = C_1^i \cdot \alpha_s(M_Z) + C_2^i \cdot {\alpha_s}^2(M_Z); \quad (4)$$

- the value of $\alpha_s(M_Z)$ was then determined by a χ^2 fit of Eq. (4) to the measured $d\sigma/dA$ values for several regions of the variable A.

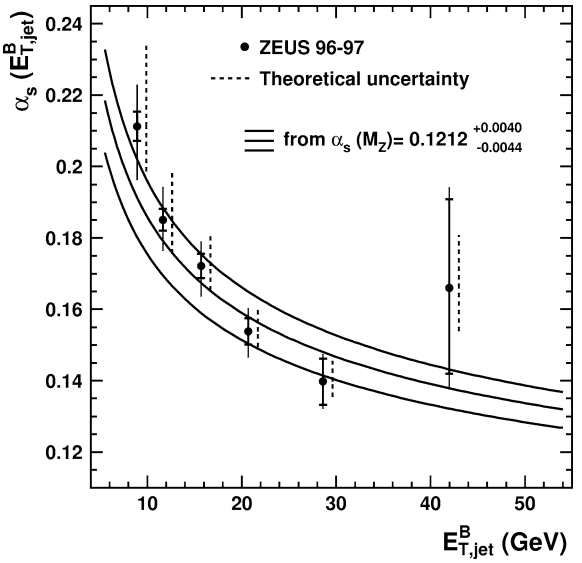

Fig. 6. The $\alpha_s(E^B_{T,\mathrm{jet}})$ values determined from the QCD fit of the measured $d\sigma/dE^B_{T,\mathrm{jet}}$ as a function of $E^B_{T,\mathrm{jet}}$. The inner error bars represent the statistical uncertainty of the data. The outer error bars show the statistical and systematic uncertainties added in quadrature. The dashed error bars display the theoretical uncertainties. The three curves indicate the renormalisation group predictions obtained from the $\alpha_s(M_Z)$ central value determined in this analysis and its associated uncertainty.

This procedure correctly handles the complete α_s dependence of the NLO differential cross sections (the explicit dependence coming from the partonic cross sections and the implicit dependence coming from the PDFs) in the fit, while preserving the correlation between α_s and the PDFs.

The uncertainty on the extracted values of $\alpha_s(M_Z)$ due to the experimental systematic uncertainties was evaluated by repeating the analysis above for each systematic check [43]. The overall normalisation uncertainty from the luminosity determination was also considered. The largest contribution to the experimental uncertainty comes from the jet energy scale.

The theoretical uncertainties, evaluated as described in Section 5, arising from terms beyond NLO, uncertainties in the proton PDFs and uncertainties in the hadronisation correction were considered. These resulted in uncertainties in $\alpha_s(M_Z)$ of 3%, 1% and 0.2%, respectively. The total theoretical uncertainty was obtained by adding these uncertainties in quadrature.

The best determination of $\alpha_s(M_Z)$ was obtained by using the measured $d\sigma/dQ^2$ for $Q^2 > 500$ GeV^2, for which both the theoretical and total uncertainties in $\alpha_s(M_Z)$ are minimised. A good fit was obtained with $\chi^2 = 2.1$ for 4 data points. The fitted value is

$$\alpha_s(M_Z) = 0.1212 \pm 0.0017(\mathrm{stat.})^{+0.0023}_{-0.0031}(\mathrm{syst.}) \\ {}^{+0.0028}_{-0.0027}(\mathrm{th.}).$$

As a cross check, the measurement was repeated using the five sets of proton PDFs of the CTEQ4 A-series [5]; the result is in good agreement with the above value. Two other determinations of $\alpha_s(M_Z)$ were performed. The first made use of the measured $d\sigma/dQ^2$ for the entire Q^2 range studied, $Q^2 > 125$ GeV^2, resulting in $\alpha_s(M_Z) = 0.1244 \pm 0.0009(\mathrm{stat.})^{+0.0034}_{-0.0041}(\mathrm{syst.})^{+0.0057}_{-0.0040}(\mathrm{th.})$. The second used the measured $d\sigma/dE^B_{T,\mathrm{jet}}$ in the region where the hadronisation corrections are small, $E^B_{T,\mathrm{jet}} > 14$ GeV, resulting in $\alpha_s(M_Z) = 0.1212 \pm 0.0013(\mathrm{stat.})^{+0.0030}_{-0.0036}(\mathrm{syst.})^{+0.0041}_{-0.0030}(\mathrm{th.})$. These results are consistent with the central value quoted above.

The value of $\alpha_s(M_Z)$ obtained is consistent with the current PDG value, $\alpha_s(M_Z) = 0.1181 \pm 0.0020$ [50] and recent determinations by the H1 [21] and ZEUS [17,19] Collaborations. It is compatible with a recent determination from the measurement of the inclusive jet cross section in $p\bar{p}$ collisions at $\sqrt{s} = 1800$ GeV, $\alpha_s(M_Z) = 0.1178 \pm 0.0001(\mathrm{stat.})^{+0.0081}_{-0.0095}(\mathrm{syst.})^{+0.0092}_{-0.0075}(\mathrm{th.})$ [51]. It is in agreement with, and has a precision comparable to, the most accurate value obtained in e^+e^- interactions [46].

The QCD prediction for the energy-scale dependence of the strong coupling constant has been tested by determining α_s from the measured differential cross sections at different scales. Since the NLO QCD calculations with $\mu_R = E^B_{T,\mathrm{jet}}$ provide a better description of the data than those using $\mu_R = Q$, a QCD fit to the measured $d\sigma/dE^B_{T,\mathrm{jet}}$ was performed in each bin of $E^B_{T,\mathrm{jet}}$. The principle of the fit is the same as outlined above, with the only difference being that the α_s dependence of $d\sigma/dE^B_{T,\mathrm{jet}}$ in Eq. (4) was parameterised in terms of $\alpha_s(\langle E^B_{T,\mathrm{jet}}\rangle)$ rather than $\alpha_s(M_Z)$, where $\langle E^B_{T,\mathrm{jet}}\rangle$ is the mean value of $E^B_{T,\mathrm{jet}}$ in each bin. The measured $\alpha_s(\langle E^B_{T,\mathrm{jet}}\rangle)$ values, with their experimental and theoretical systematic uncertainties estimated as for $\alpha_s(M_Z)$, are shown in Fig. 6. The measure-

ments are compared with the renormalisation group predictions obtained from the $\alpha_s(M_Z)$ central value determined above and its associated uncertainty. The results are in good agreement with the predicted running of the strong coupling constant over a large range in $E^B_{T,\mathrm{jet}}$.

10. Summary

Measurements of the differential cross sections for inclusive jet production in neutral current deep inelastic e^+p scattering at a centre-of-mass energy of 300 GeV have been presented. The cross sections refer to jets of hadrons identified with the longitudinally invariant k_T cluster algorithm in the Breit frame. The cross sections are given in the kinematic region $Q^2 > 125$ GeV^2 and $-0.7 < \cos\gamma < 0.5$.

NLO QCD calculations provide a good description of the measured differential cross sections for inclusive jet production at high Q^2, $Q^2 > 500$ GeV^2, or high jet transverse energies, $E^B_{T,\mathrm{jet}} > 14$ GeV. This observation complements and extends that of the exclusive dijet cross section to lower Q^2. At low Q^2 and low jet transverse energies, differences of $\sim$10% between data and calculations are observed, which are of the same size as the theoretical uncertainties.

A QCD fit of the measured cross section as a function of Q^2 for $Q^2 > 500$ GeV^2 yields

$$\alpha_s(M_Z) = 0.1212 \pm 0.0017(\mathrm{stat.})^{+0.0023}_{-0.0031}(\mathrm{syst.}) \; {}^{+0.0028}_{-0.0027}(\mathrm{th.}).$$

This value is in good agreement with the world average and is at least as precise as any other individual measurement.

Acknowledgements

We thank the DESY Directorate for their strong support and encouragement. The remarkable achievements of the HERA machine group were essential for the successful completion of this work and are greatly appreciated. We are grateful for the support of the DESY computing and network services. The design, construction and installation of the ZEUS detector have been made possible owing to the ingenuity and effort of many people from DESY and home institutes who are not listed as authors.

References

[1] V.N. Gribov, L.N. Lipatov, Sov. J. Nucl. Phys. 15 (1972) 438;
L.N. Lipatov, Sov. J. Nucl. Phys. 20 (1975) 94;
G. Parisi, in: J. Tran Thanh Van (Ed.), in: Proceedings of the 11th Rencontre de Moriond, Vol. 3, Flaine, France, 1976, p. 83;
Yu.L. Dokshitzer, Sov. Phys. JETP 46 (1977) 641;
G. Altarelli, G. Parisi, Nucl. Phys. B 126 (1977) 298.
[2] L.W. Whitlow, et al., Phys. Lett. B 282 (1992) 475;
BCDMS Collaboration, A.C. Benvenuti, et al., Phys. Lett. B 223 (1989) 485;
BCDMS Collaboration, A.C. Benvenuti, et al., Phys. Lett. B 237 (1990) 592;
NMC Collaboration, M. Arneodo, et al., Nucl. Phys. B 483 (1997) 3;
NMC Collaboration, M. Arneodo, et al., Nucl. Phys. B 487 (1997) 3;
E665 Collaboration, M.R. Adams, et al., Phys. Rev. D 54 (1996) 3006;
CCFR Collaboration, W.G. Seligman, et al., Phys. Rev. Lett. 79 (1997) 1213;
FNAL E866/NuSea Collaboration, E.A. Hawker, et al., Phys. Rev. Lett. 80 (1998) 3715.
[3] H1 Collaboration, S. Aid, et al., Nucl. Phys. B 470 (1996) 3;
H1 Collaboration, C. Adloff, et al., Eur. Phys. J. C 21 (2001) 33;
ZEUS Collaboration, M. Derrick, et al., Z. Phys. C 72 (1996) 399;
CDF Collaboration, F. Abe, et al., Phys. Rev. Lett. 81 (1998) 5754.
[4] ZEUS Collaboration, S. Chekanov, et al., Eur. Phys. J. C 21 (2001) 443.
[5] H.L. Lai, et al., Phys. Rev. D 55 (1997) 1280.
[6] J. Pumplin, et al., JHEP 0207 (2002) 012.
[7] M. Glück, E. Reya, A. Vogt, Z. Phys. C 67 (1995) 433;
M. Glück, E. Reya, A. Vogt, Eur. Phys. J. C 5 (1998) 461.
[8] A.D. Martin, et al., Eur. Phys. J. C 4 (1998) 463;
A.D. Martin, et al., Eur. Phys. J. C 14 (2000) 133.
[9] A.D. Martin, et al., Eur. Phys. J. C 23 (2002) 73.
[10] M. Botje, Eur. Phys. J. C 14 (2000) 285.
[11] R.P. Feynman, Photon–Hadron Interactions, Benjamin, New York, 1972;
K.H. Streng, T.F. Walsh, P.M. Zerwas, Z. Phys. C 2 (1979) 237.
[12] S. Catani, et al., Nucl. Phys. B 406 (1993) 187.
[13] B.R. Webber, J. Phys. G 19 (1993) 1567.
[14] M. Klasen, G. Kramer, Phys. Lett. B 366 (1996) 385;
S. Frixione, G. Ridolfi, Nucl. Phys. B 507 (1997) 315;
B. Poetter, Comput. Phys. Commun. 133 (2000) 105.
[15] S. Catani, M.H. Seymour, Nucl. Phys. B 485 (1997) 291;
S. Catani, M.H. Seymour, Nucl. Phys. B 510 (1998) 503, Erratum.

[16] ZEUS Collaboration, S. Chekanov, et al., Eur. Phys. J. C 23 (2002) 13.
[17] ZEUS Collaboration, J. Breitweg, et al., Phys. Lett. B 507 (2001) 70.
[18] ZEUS Collaboration, M. Derrick, et al., Phys. Lett. B 363 (1995) 201.
[19] ZEUS Collaboration, S. Chekanov, et al., Preprint DESY-02-105, DESY, 2002, submitted to Phys. Rev. D.
[20] H1 Collaboration, T. Ahmed, et al., Phys. Lett. B 346 (1995) 415;
H1 Collaboration, C. Adloff, et al., Eur. Phys. J. C 5 (1998) 625;
H1 Collaboration, C. Adloff, et al., Eur. Phys. J. C 6 (1999) 575.
[21] H1 Collaboration, C. Adloff, et al., Eur. Phys. J. C 19 (2001) 289.
[22] ZEUS Collaboration, M. Derrick, et al., Phys. Lett. B 293 (1992) 465.
[23] ZEUS Collaboration, U. Holm (Ed.), The ZEUS Detector, Status Report (unpublished), DESY, Hamburg, 1993, available on: http://www-zeus.desy.de/bluebook/bluebook.html.
[24] N. Harnew, et al., Nucl. Instrum. Methods A 279 (1989) 290;
B. Foster, et al., Nucl. Phys. Proc. Suppl. B 32 (1993) 181;
B. Foster, et al., Nucl. Instrum. Methods A 338 (1994) 254.
[25] M. Derrick, et al., Nucl. Instrum. Methods A 309 (1991) 77;
A. Andresen, et al., Nucl. Instrum. Methods A 309 (1991) 101;
A. Caldwell, et al., Nucl. Instrum. Methods A 321 (1992) 356;
A. Bernstein, et al., Nucl. Instrum. Methods A 336 (1993) 23.
[26] J. Andruszków, et al., Report DESY-92-066, DESY, 1992;
ZEUS Collaboration, M. Derrick, et al., Z. Phys. C 63 (1994) 391;
J. Andruszków, et al., Acta Phys. Pol. B 32 (2001) 2025.
[27] ZEUS Collaboration, J. Breitweg, et al., Eur. Phys. J. C 8 (1999) 367.
[28] H. Abramowicz, A. Caldwell, R. Sinkus, Nucl. Instrum. Methods A 365 (1995) 508.
[29] S. Bentvelsen, J. Engelen, P. Kooijman, in: W. Buchmüller, G. Ingelman (Eds.), Proc. Workshop on Physics at HERA, October 1991, Vol. 1, DESY, Hamburg, 1992, p. 23.
[30] S.D. Ellis, D.E. Soper, Phys. Rev. D 48 (1993) 3160.
[31] J.E. Huth, et al., in: E.L. Berger (Ed.), Research Directions for the Decade, Proceedings of Summer Study on High Energy Physics, 1990, World Scientific, Singapore, 1992, also in preprint FERMILAB-CONF-90-249-E.
[32] R. Brun et al., GEANT3, Technical Report CERN-DD/EE/84-1, CERN, 1987.
[33] G. Ingelman, A. Edin, J. Rathsman, Comput. Phys. Commun. 101 (1997) 108.
[34] A. Kwiatkowski, H. Spiesberger, H.-J. Möhring, Comput. Phys. Commun. 69 (1992) 155, also in: Proc. Workshop Physics at HERA, DESY, Hamburg, 1991;
H. Spiesberger, An Event Generator for *ep* Interactions at HERA Including Radiative Processes (Version 4.6), 1996, available on: http://www.desy.de/~hspiesb/heracles.html.
[35] K. Charchuła, G.A. Schuler, H. Spiesberger, Comput. Phys. Commun. 81 (1994) 381;
H. Spiesberger, HERACLES and DJANGOH: Event Generation for *ep* Interactions at HERA Including Radiative Processes, 1998, available on: http://www.desy.de/~hspiesb/djangoh.html.
[36] Y. Azimov, et al., Phys. Lett. B 165 (1985) 147;
G. Gustafson, Phys. Lett. B 175 (1986) 453;
G. Gustafson, U. Pettersson, Nucl. Phys. B 306 (1988) 746;
B. Andersson, et al., Z. Phys. C 43 (1989) 625.
[37] L. Lönnblad, Comput. Phys. Commun. 71 (1992) 15;
L. Lönnblad, Z. Phys. C 65 (1995) 285.
[38] ZEUS Collaboration, J. Breitweg, et al., Eur. Phys. J. C 11 (1999) 251.
[39] B. Andersson, et al., Phys. Rep. 97 (1983) 31.
[40] T. Sjöstrand, Comput. Phys. Commun. 39 (1986) 347;
T. Sjöstrand, M. Bengtsson, Comput. Phys. Commun. 43 (1987) 367.
[41] R.K. Ellis, D.A. Ross, A.E. Terrano, Nucl. Phys. B 178 (1981) 421.
[42] D. Graudenz, in: B.A. Kniehl, G. Krämer, A. Wagner (Eds.), Proceedings of the Ringberg Workshop on New Trends in HERA physics, World Scientific, Singapore, 1998, hep-ph/9708362;
D. Graudenz, hep-ph/9710244.
[43] O. González, Ph.D. Thesis, U. Autónoma de Madrid, DESY-THESIS-2002-020, 2002.
[44] G. Marchesini, et al., Comput. Phys. Commun. 67 (1992) 465;
G. Corcella, et al., JHEP 0101 (2001) 010;
G. Corcella, et al., hep-ph/0107071.
[45] B.R. Webber, Nucl. Phys. B 238 (1984) 492.
[46] For a review and further discussion see: S. Bethke, J. Phys. G 26 (2000) R27.
[47] H. Raach, Ph.D. Thesis, Freiburg U., DESY-THESIS-2001-046, 2001.
[48] ZEUS Collaboration, S. Chekanov, et al., Phys. Lett. B 531 (2002) 9;
ZEUS Collaboration, S. Chekanov, et al., Eur. Phys. J. C 23 (2002) 615;
M. Wing, (on behalf of the ZEUS Collaboration), in: Proceedings for 10th International Conference on Calorimetry in High Energy Physics, hep-ex/0206036.
[49] ZEUS Collaboration, J. Breitweg, et al., Eur. Phys. J. C 11 (1999) 427.
[50] Particle Data Group, D.E. Groom, et al., Eur. Phys. J. C 15 (2000) 1.
[51] CDF Collaboration, T. Affolder, et al., Phys. Rev. Lett. 88 (2002) 042001.